

Fabrication of a Thin-film Capacitive Force Sensor Array for Tactile Feedback in Robotic Surgery

Omeed H. Paydar, Christopher R. Wottawa, Richard E. Fan, Erik P. Dutson, Warren S. Grundfest, Martin O. Culjat, Rob N. Candler

Abstract— Although surgical robotic systems provide several advantages over conventional minimally invasive techniques, they are limited by a lack of tactile feedback. Recent research efforts have successfully integrated tactile feedback components onto surgical robotic systems, and have shown significant improvement to surgical control during *in vitro* experiments. The primary barrier to the adoption of tactile feedback in clinical use is the unavailability of suitable force sensing technologies. This paper describes the design and fabrication of a thin-film capacitive force sensor array that is intended for integration with tactile feedback systems. This capacitive force sensing technology could provide precise, high-sensitivity, real-time responses to both static and dynamic loads. Capacitive force sensors were designed to operate with optimal sensitivity and dynamic range in the range of forces typical in minimally invasive surgery (0 – 40 N). Initial results validate the fabrication of these capacitive force-sensing arrays. We report 16.3 pF and 146 pF for 1-mm² and 9-mm² capacitive areas, respectively, whose values are within 3% of theoretical predictions.

I. INTRODUCTION

Robotic minimally invasive surgery offers advantages such as improved range of motion, enhanced visualization, and higher precision compared to standard laparoscopic techniques. However, there is no direct contact between surgeon and patient. As a result, there is a complete lack of tactile feedback as well as minimal kinesthetic feedback (which limits tool collision and over-extension of joints, but does not prevent damage to tissues or sutures).

Tactile feedback systems utilize sensory substitution or sensory augmentation to provide tactile information that was

Manuscript received March 29, 2012. This work was supported in part by the Telemedicine and Advanced Technology Research Center (TATRC) / Department of Defense under Grant W81XWH-07-1-0672.

O.H Paydar is with the UCLA Biomedical Engineering Interdepartmental Program (BME IDP), the Sensors & Technology Laboratory (STL), and the Center for Advanced Surgical and Interventional Technology (CASIT) at UCLA, Los Angeles, CA 90095 USA (phone: 310-825-0585; email: omeed.paydar@ucla.edu).

C.R. Wottawa is with the BME IDP and CASIT, Los Angeles, CA 90095 USA.

R.E. Fan and E.P. Dutson are with the UCLA Department of Surgery and CASIT, Los Angeles, CA 90095 USA.

W.S. Grundfest and M.O Culjat are with the UCLA Departments of Bioengineering and Surgery and CASIT, Los Angeles, CA 90095 USA.

R.N. Candler is with the UCLA Department of Electrical Engineering, the California NanoSystems Institute (CNSI), CASIT, and STL, Los Angeles, CA 90095 USA.

previously attenuated or unavailable to the user. This task can be accomplished by applying mechanical deformations to the user's skin, thereby activating sensory mechanoreceptors. These systems have potential application in surgical and industrial robotics, virtual reality, gaming applications, and rehabilitation.

A robotic surgery tactile feedback system was previously developed by our group and integrated onto the da Vinci surgical system. It measures contact forces at robotic grasper tips, and displays this information to a surgeon's fingertips by inflating balloon actuators mounted on the master controls.[1] Using this system, our group discovered that tactile feedback produced a significant reduction in grip forces during simple surgical tasks.[2] (Figure 1) Additional experiments using an array-based system demonstrated that spatial information could accurately be perceived by the user.[3] Further use of this system in evaluating tactile feedback is ultimately limited by the lack of a robust, and low profile sensor array that is capable of withstanding both sterilization and wet, *in vivo* environments.

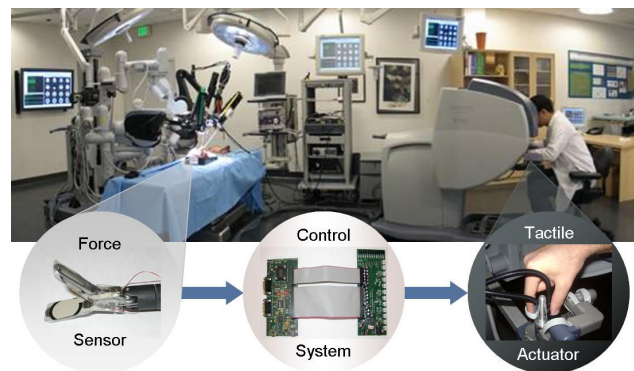


Figure 1. Tactile feedback system measures contact forces at grasper tips, and displays this information to surgeon's fingertip by inflating balloon actuators.

In robotic surgery, force-sensing systems are primarily constrained by small mounting surfaces; the da Vinci Cadiere graspers, which are among the largest instruments, have a contact area of 5 mm x 14 mm, and an end-effector thickness of 3 mm. In addition, force sensors used during robotic surgery must exhibit minimal hysteresis and have an appropriate dynamic range. Forces felt by surgical tools are typically in the 0–5 N range, but have been reported as high as 40 N, and over an average duration of 2-3 s.[4] There are

several additional constraints that are specific to use in the clinic. Sensors must survive wet, *in-vivo* environments, be biocompatible, have quick response time, survive the temperatures and pressures of autoclave sterilization, be non-reactive with chemical methods (such as ethylene oxide), and not interfere or be interfered with by nearby electrocautery devices.

Many technologies, including capacitive, piezoresistive, and piezoelectric sensing modalities, are strong candidates for thin-film force sensing and have been used in research prototypes.[5-14] Commercially available technologies do not meet the size constraints of current minimally invasive surgical equipment as well as the precision necessary for use in surgical operation.[15]

Piezoresistive sensors make use of semiconductive materials' property of changing electrical resistance when under mechanical strain. When combined with a voltage driving circuit, changes in applied force can be converted to changes in output voltage. There are many different types of piezoresistive sensor designs. Geometries include membrane designs (strain gauge) and sandwich designs. High stiffness semiconductor materials (polysilicon), doped elastomers, and commercial piezoresistive pastes have all been used as piezoresistive substrates. Piezoresistive sensors are cited as having disadvantages of nonlinear responses, hysteresis, the need to optimize the mechanical and electrical configurations of the piezoresistive elastomer, and a high dependence on temperature. Advantages include wide dynamic range, and durability.

Piezoelectric sensors differ from piezoresistive sensors in that certain materials, such as polyvinylidene fluoride (PVDF) or lead zirconate titanate (PZT), will generate a voltage when under an applied load. However, with the application of a constant load, the piezoelectric sensor output quickly decays; therefore these types of sensors are most suited towards measuring dynamic force, rather than static force.

Additional methods of measuring force include a fluid filled elastomeric skin, optical sensors, and inductive sensor technologies. These methods sometimes have thick size requirements, high complexity (moving parts), and interference to and from electrocautery systems that are commonly used during surgery. Many commercial load cells and strain gauges are also available, but are not practical for surgical robotics.

The capacitive force sensors discussed here utilize a spring-like dielectric positioned between two conducting plates. The applied force compresses the dielectric, altering the distance between the plates and thus changing the capacitance. Circuitry measures this capacitance and translates it into the force differential. Generally, advantages associated with capacitive sensors are high sensitivity and precision. Typical capacitive sensors can have a very low detectable range: <1 pF for 0 – 20 N. However,

improvements in the resolution of commercial measurement electronics as well as microelectromechanical systems (MEMS) fabrication techniques that allow for thinner dielectric layers have made this type of sensor feasible for thin-film force measurement.

This paper presents the design, fabrication, and characterization of a scalable thin-film capacitive force sensor array. This device, when packaged and integrated with surgical robotic systems, is expected to allow tactile feedback to be extended for the first time to *in vivo* settings

II. DEVICE DESIGN

Our microfabricated parallel plate capacitor consists of two conductive elements (plates) separated by a pliant dielectric with relative permittivity, ϵ_r . Neglecting fringing fields, the capacitance is defined by equation 1.

$$C = \frac{\epsilon_0 \cdot \epsilon_r \cdot A_{plate}}{z} \quad (1)$$

The permittivity of free space, ϵ_0 , equals $8.85 \times 10^{-12} \text{ F}\cdot\text{m}^{-1}$. To avoid saturation of the measurement circuitry the area, A_{plate} , and plate separation, z , were constrained. Elastic deformation of the sensor by compressive loads reduces the gap between the capacitor plates. This deformation is defined as,

$$\frac{\partial z}{\partial F} = -\frac{z}{E \cdot A_{plate}} \quad (2)$$

The deformation is a function of the initial separation, z , the elastic modulus, E , and the plate area. Consequently, the sensitivity of the device is,

$$\frac{\partial C}{\partial F} = -\frac{\epsilon}{E \cdot z} \quad (3)$$

where ϵ represents the product of the material dielectric constant and the permittivity of free space.

In vivo implementation of the sensor array necessitates material biocompatibility. The material selection is also guided by the electrical properties, such as relative permittivity and resistivity. To satisfy both compatibility and electrical constraints, we chose to fabricate the devices with gold capacitor plates and Parylene C as the insulating dielectric material.

III. SENSOR ARRAY FABRICATION

Fabrication of the capacitive sensor array was accomplished by established MEMS processes. The substrates, 4-inch glass wafers, were placed in piranha solution, 3:1 mixture of concentrated H_2SO_4 to 30% H_2O_2 , to remove organic residue and contaminants (Figure 2.1). Next, negative tone lift-off photoresist (nLOF 2020) was spun on the wafer and patterned to define the bottom metal layer. A

20-nm/100-nm Cr/Au stack was evaporated onto the wafers. The 20-nm chromium layer is necessary to improve the adhesion of the thicker gold layer to the wafer surface. The bottom metal pattern was defined after lift-off in acetone (Figure 2.2). Next, the wafer was prepared for chemical vapor deposition (CVD) of Parylene C ($\epsilon_r = 3.1$ at 1 kHz) at a designed 2.0 μm thickness (Figure 2.3). Visual inspection (RI = 1.64) and profilometric measurement verified a 1.73- μm parylene layer. A thick positive tone photoresist (SPR 220-7.0) was spun and patterned to mask an etch through the parylene using a reactive ion etch (RIE) tool. This etch allows electrical access to the bottom electrode, which is under the parylene (Figure 2.4). A final lithography of negative-tone photoresist (Figure 2.5) defines the pattern for a second evaporated 20-nm/100 nm Cr/Au stack. Again, acetone lift-off shapes the top capacitor plate and completes the fabrication process (Figure 2.6).

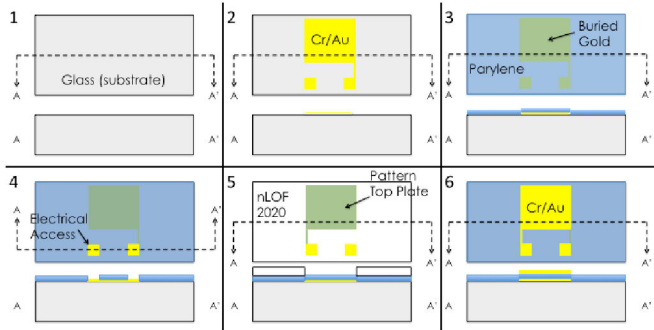


Figure 2. Process flow of the capacitive sensor design. Fabrication of the arrays was accomplished with established microfabrication processes and tools. The illustration is of a single capacitor within the capacitive sensor array. Each panel depicts a top view (top) and cross section (bottom) through the dashed A-A' line.

The mounting surface of the da Vinci Cadiere grasper limits the number and dimensions of the capacitor arrays. Fabrication of 2x3 and 2x4 arrays of 1- mm^2 capacitors and single 9- mm^2 capacitors were designed on the wafer for initial validation of the sensor array.

IV. DEVICE CHARACTERIZATION

Successful array fabrication and initial characterization of the sensor performance were validated by impedance measurements (Agilent 4294A). Of note, the series resistance—a result of the fabricated capacitor non-idealities—decays at higher frequencies. Because of the sensing circuitry, this frequency-dependent series resistance requires further analysis prior to implementing the arrays on chip.

The high-power reactive ion etch responsible for opening the vias and exposing the bond pads roughens the unprotected metal surface—this has a negligible effect to wirebond adhesion. Pad areas with residual parylene are not subject to surface roughening and retain the gold luster at the expense of the available bonding surface (Figure 3).

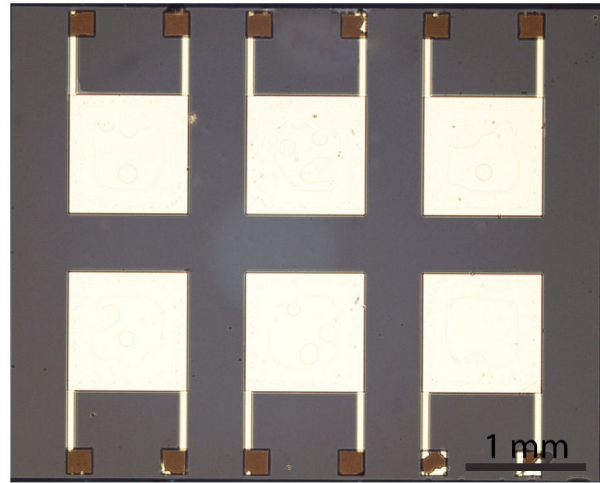


Figure 3. Microfabricated 2x3 capacitor array. A Cr/Au stack defines each of the 1- mm^2 metal layers and Parylene C constitutes the sandwiched dielectric. Roughened bond pad surfaces appear darker than the protected gold. This effect does not prevent wirebond adhesion.

A 1- V_{pp} signal swept from 1 kHz to 20 kHz applied to the sensor array was used to characterize the uncompressed, baseline series resistance and capacitance. The dependence of the dielectric constant on frequency accounts for the decrease in capacitance at higher frequencies.

Experimental results for 9- mm^2 and 1- mm^2 capacitors are presented in (Figure 4) and (Figure 5), respectively.

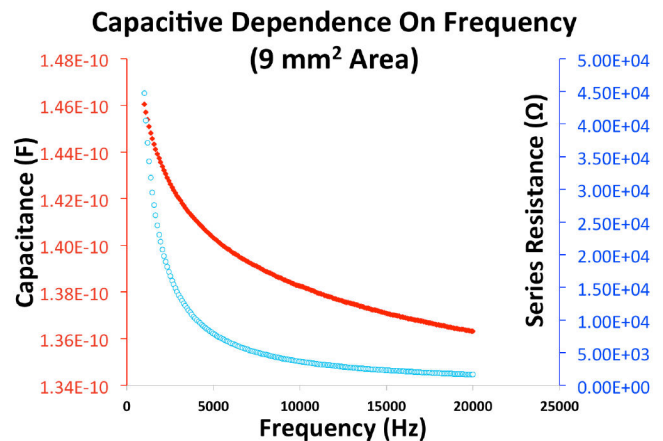


Figure 4. Experimental capacitance (square data points) measurements for 9- mm^2 devices. The decay in the capacitance is a function of the frequency dependent dielectric constant. The results match theory closely—2.1% error. The series resistance (circular data points) is frequency-dependent. At 20 kHz, the series resistance decays to 3.7% of the initial measurement.

The 1 kHz capacitance of the 9- mm^2 sample was reported at 146 pF (2.1% error). Similarly, the experimentally determined capacitance of the 1- mm^2 capacitor was determined to be 16.3 pF (2.5% error).

Calculated capacitances, at 1 kHz, confirm the experimental results and validate the device fabrication 143 pF (9 mm^2) and 15.9 pF (1 mm^2) with 1.73 μm plate separation. Force calibrations are underway to verify the sensitivity calculations.

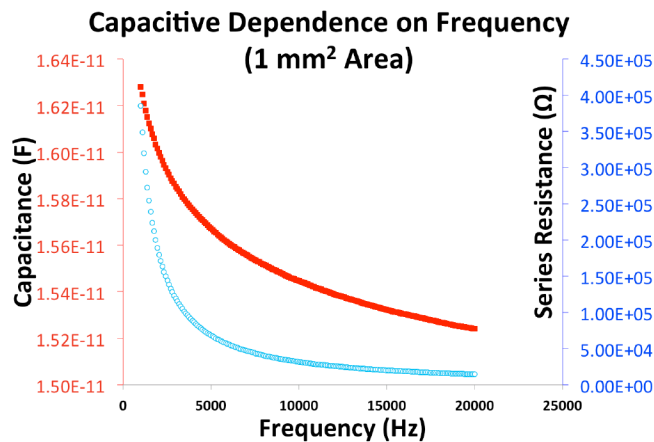


Figure 5. Experimental capacitance (square data points) measurements for 1-mm² devices. The decay in the capacitance is a function of the frequency dependent dielectric constant. The results match theory closely—2.5% error. The series resistance (circular data points) is frequency-dependent. At 20 kHz, the series resistance decays to 3.8% of the initial measurement.

V. CONCLUSION

Thin-film capacitive sensors provide a miniaturized, low profile, biocompatible solution for measuring forces as part of a tactile feedback system for minimally invasive surgery. Capacitance measurements from the completed capacitive arrays agree with theory and validate the fabrication process. The results of the device fabrication demonstrate a potential solution for *in vivo* force sensing.

ACKNOWLEDGMENTS

The authors would like to thank the Nanoelectronics Research Facility (NRF) and the Integrated Systems Nanofabrication Cleanroom (ISNC) in the California NanoSystems Institute (CNSI) at UCLA for making fabrication of the devices possible. We would also like to express our gratitude to Joe Zendejas for fruitful discussions.

REFERENCES

- ¹ Culjat MO, King CH, Franco ML, Lewis CE, Bisley JW, Dutson EP, Grundfest WS (2008) A Tactile feedback system for robotic surgery. Proceedings on the IEEE Engineering in Medicine and Biology Society 1:1930-1934
- ² King CH, Culjat MO, Franco ML, Lewis CE, Dutson EP, Grundfest WS, Bisley JW (2009) Tactile feedback induces reduced grasping force in robotic surgery. IEEE Transactions on Haptics
- ³ Franco ML, King CH, Culjat MO, Lewis CE, Bisley JW, Holmes EC, Grundfest WS, Dutson EP (2009) An integrated pneumatic tactile feedback actuator array for robotic surgery. International Journal of Medical Robotics and Computer-Assisted Surgery 5(1):13-19
- ⁴ Brown JD, Rosen J, Chang L, Sinanan MN, Hannaford B, "Quantifying surgeon grasping mechanics in laparoscopy using the blue DRAGON system," Studies in Health Technology and Informatics – Medicine Meets Virtual Reality, Newport Beach, CA, January 2004.
- ⁵ Nicholls HR, Lee MH, "A survey of robot tactile sensing technology", Int. J Robotics Research 1989;8(3):3-30
- ⁶ Patel P. Synthetic Skin Sensitive to the Lightest Touch. Article. IEEE Spectrum. September 2010.
- ⁷ Tekscan: Tactile Pressure Measurement, Pressure Mapping Systems, and Force Sensors and Measurement Systems. <http://www.tekscan.com/> Accessed Sept. 23, 2009.
- ⁸ Najarian S, Dargahi J, Mehrizi AA. Artificial Tactile Sensing in Biomedical Engineering. McGraw-Hill Biophotonics 2009.
- ⁹ Pressure Profile Systems. <http://www.pressureprofile.com/> Accessed Sept. 23 2009
- ¹⁰ Schostek S, Ho N, Kalanovic D, Schurr MO (2006) Artificial tactile sensing in minimally invasive surgery – a new technical approach. Minim Invasive Ther Allied Technol 15(5):296-304
- ¹¹ Palasagaram JN, Ramadoss R. MEMS Capacitive Pressure Sensor Array fabricated Using Printed Circuit Processing Technologies. 32nd Annual Conference of IEEE Industrial Electronics Society 2005 IECON 2005
- ¹² Wettels N, Santos VJ, Johansson RS, Loeb GE. Biomimetic Tactile Sensor Array. Advanced Robotics 22 (2008) 829-849.
- ¹³ Schostek S, Schurr MO, Buess GF. Review on aspects of artificial tactile feedback in laparoscopic surgery. (In Press) Medical Engineering and Physics (2009).
- ¹⁴ Maheshwari V, Saraf R. "Tactile Devices To Sense Touch on a Par with a Human Finger." Chem. Int. Ed. 2008, 47, 7808-7826.
- ¹⁵ Buess GF, Schurr MO, Fischer SC. Robotics and allied technologies in endoscopic surgery. Arch Surg. 2000; 135:229-235.